PHOTOMETRY OF 25 LARGE MAIN-BELT ASTEROIDS WITH TRAPPIST-NORTH AND -SOUTH

Marin Ferrais, Pierre Vernazza, Laurent Jorda
Aix Marseille Université, CNRS, LAM, Laboratoire d'Astrophysique de Marseille, Marseille, France
marin.ferrais@lam.fr

Emmanuël Jehin, Francisco J. Pozuelos, Jean Manfroid
Space sciences, Technologies & Astrophysics Research (STAR) Institute
Université de Liège
Allée du 6 Août 19, 4000 Liège, Belgium

Youssef Moulane
Physics Department, Auburn University, AL 36832, USA

Khalid Barkaoui
Astrobiology Research Unit, Université de Liège, Allée du 6 Août 19C, 4000 Liège, Belgium
Department of Earth, Atmospheric and Planetary Science, Massachusetts Institute of Technology, 77 Massachusetts Avenue, Cambridge, MA 02139, USA
Instituto de Astrofísica de Canarias (IAC), Vía Láctea, 38205 La Laguna, Tenerife, Spain

Zouhair Benkhaldoun
Oukaïmenden Observatory,
Cadi Ayyad University, Marrakech, Morocco

(Received: 2022 June 8)

Densely sampled lightcurves of 25 large main-belt asteroids were obtained with the TRAPPIST-South (TS) and TRAPPIST-North (TN) telescopes from 2017 to 2021. Those observations took place in support of an ESO large program aiming at observing a representative sample of large asteroids with the ESO VLT for precise shape determination from adaptive optics high-resolution imaging. Synodic rotation periods and lightcurve amplitudes have been determined for all but one target. Six asteroids were observed during two different apparitions. The data have been submitted to the ALCDEF database.

Observations were acquired with the robotic telescopes TRAPPIST-North (TN, Z53) and TRAPPIST-South (TS, I40) of the Liège University (Jehin et al., 2011). They are located, respectively, at the Oukaïmeden Observatory in Morocco and the ESO La Silla Observatory in Chile. Both are 0.6-m Ritchey-Chrétien telescopes operating at f/8 on German Equatorial mounts. The TN camera is an Andor IKONL BEX2 DD (0.60 arcsec/pixel) and the one of TS is an FLI ProLine 3041-BB (0.64 arcsec/pixel).

The raw images were calibrated with corresponding flat fields, bias, and dark frames, and photometric measurements were obtained using *IRAF* (Tody, 1986) scripts. The differential photometry and lightcurves were made with Python scripts. All the stars with a high enough SNR were used and checked to discard the variable stars for the differential photometry. Various apertures were tested to maximize the SNR. The absolute calibration in the Johnson-Cousins Rc band was then performed using the *Photometry Pipeline* developed by Mommert (2017). This pipeline allows photometric zero-point calibration by matching field stars with catalogs. The photometric catalogs PanSTARRS DR1 and SDSS-R9 were used to match up to 100 stars with solar colors for each image. The rotation periods were determined with the software *Peranso* (Vanmunster, 2018), which implements the FALC algorithm (Harris et al., 1989).

The ESO large program (ID 199.C-0074; PI P. Vernazza) supported by these observations acquired high angular resolution images of 42 large (D > 100km) main-belt asteroids with the adaptive optics instrument (AO) SPHERE at the VLT. It aimed mainly at reconstructing the 3D shape, and therefore density of those bodies to better constrain their formation and evolution. Multiple 3D reconstruction algorithms were used, notably *ADAM* and *SAGE* (Viikinkoski et al., 2015; Bartczak and Dudzinski, 2018). They combine the AO images with data from other sources, most importantly photometric lightcurves, which help to cover the viewing geometries not seen by the AO images. The final results of the program were recently published in Vernazza et al. (2021).

In the lightcurves below the Rc magnitude is plotted as a function of the rotational phase using the period indicated on the plot. The zero phase corresponds to the maximum of the curve and to the Julian Date indicated on the plot (JDo). The solid black line represents a Fourier fit up to an order indicated in the legend, and from which are computed the residuals shown in the bottom panel. The reported amplitude is from the Fourier model curve. For all our targets, the derived synodic periods agreed with previously published results found in the asteroid lightcurve database (LCDB; Warner et al., 2009). All data have been submitted to the ALCDEF database.

7 Iris is an S-type asteroid and the fourth brightest main-belt object due to its bright surface (albedo ~0.28) and small distance from the Sun. It was observed at an angular size of 0.33 arcsec by SPHERE in 2017, revealing its cratered surface (Hanuš et al., 2019). We observed it in 2020 at V ~9 mag.

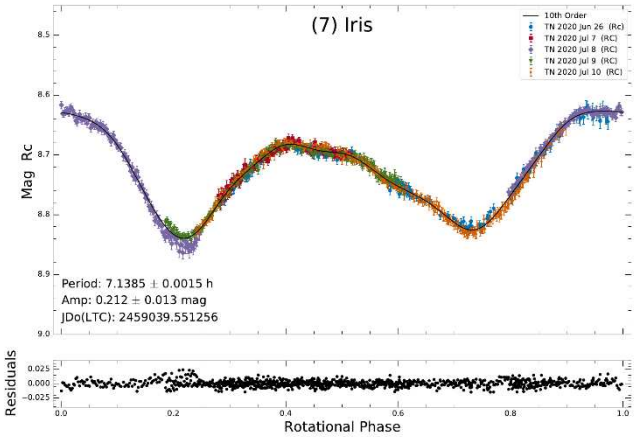

13 Egeria. The whole rotation (period of ~7h) of this Ch-type asteroid was covered in one night with TS in 2019 Aug 19.

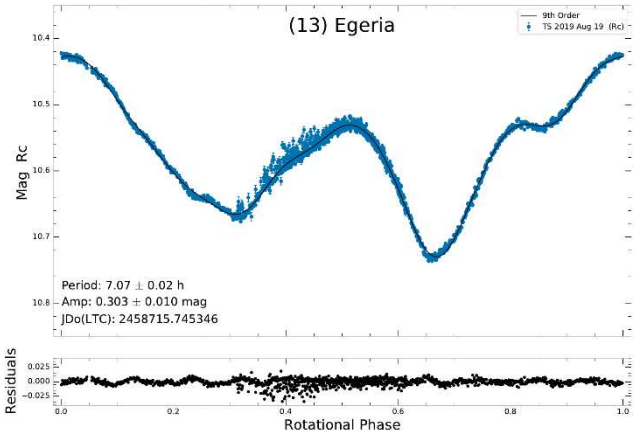

15 Eunomia is an S-type asteroid featuring an elongated shape resulting in the large observed amplitude of the lightcurve of ~0.46 mag while it was in equator-on viewing configuration.

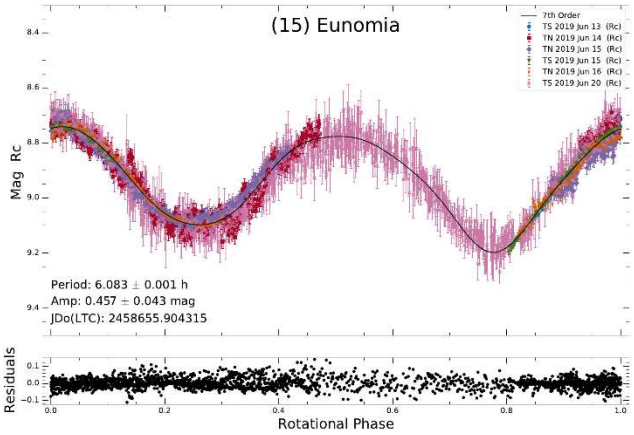

16 Psyche is a very interesting object that will be explored in-situ by a NASA space mission in 2026 (Elkins-Tanton et al., 2017). Psyche has an M-type classification, features metal at its surface and is one of the densest large asteroids known (Ferrais et al., 2020). We observed it in 2018 while it was viewed from its north pole. This explains the small amplitude of the lightcurve that shows only one maximum.

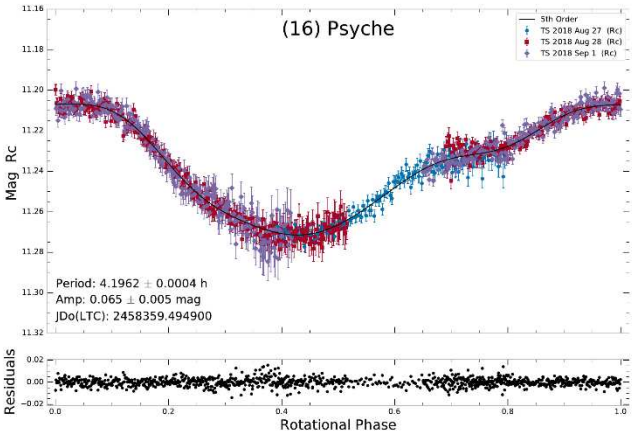

18 Melpomene is an S-type asteroid and is another example of a relatively large amplitude with ~0.3 mag.

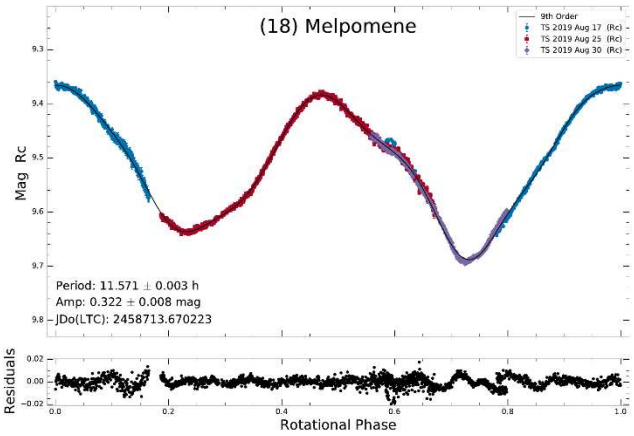

20 Massalia. We observed this S-type asteroid in 2017 and then for another night in 2019. Its rotation period is very close to 8 h, making it challenging to cover the whole rotation with data from consecutive nights. In this context, the combination of observations from both TN and TS was highly beneficial.

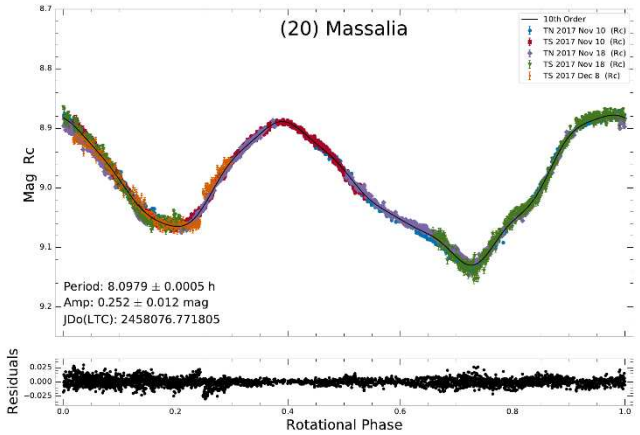

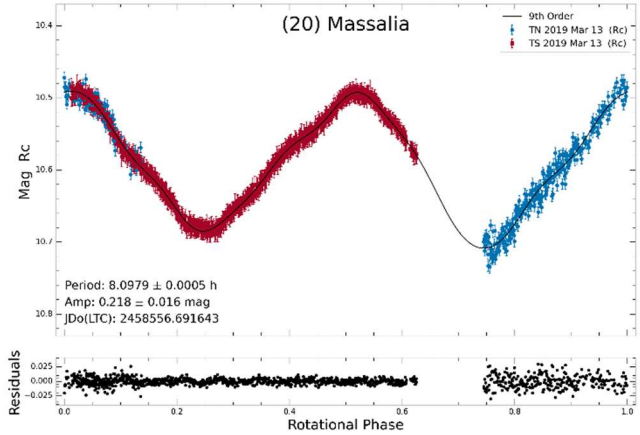

21 Lutetia was the second smallest object of our program (D = 98 km) but was visited by the ESA Rosetta space mission during its journey to comet 67P/C-G (Sierks et al., 2011). We covered the rotation on 2019 Sep. 11 using both TN and TS.

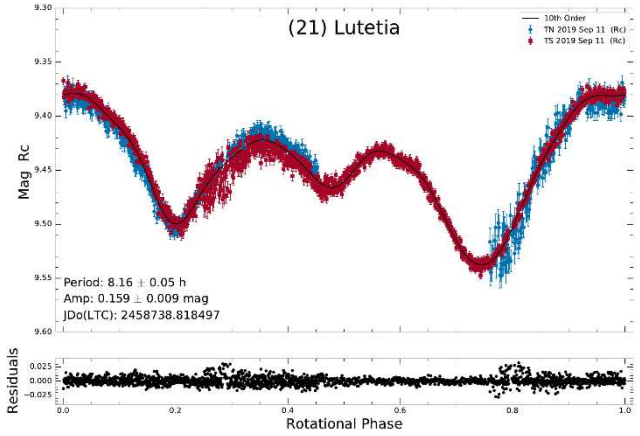

22 Kalliope is a dense M-type asteroid with a probably differentiated interior (Ferrais et al., 2022) and a relatively large companion 28 km in diameter named Linus. Our observations in 2018 were almost pole-on which explains the practically flat lightcurve.

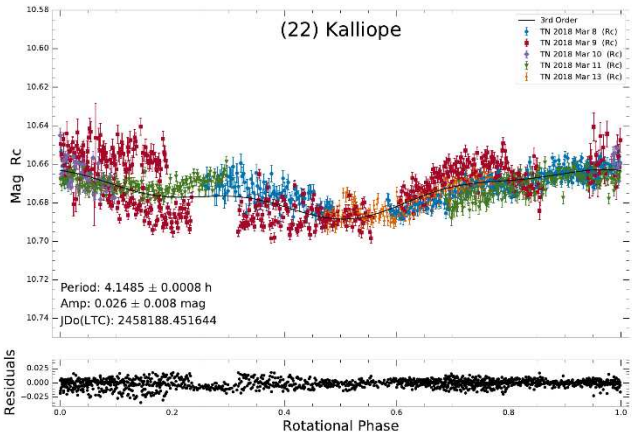

24 Themis is a carbonaceous asteroid and the parent body of one of the largest family. Themis has a relatively spherical shape which resulted in lightcurves of modest amplitudes featuring many bumps for both our 2017 and 2019 observations.

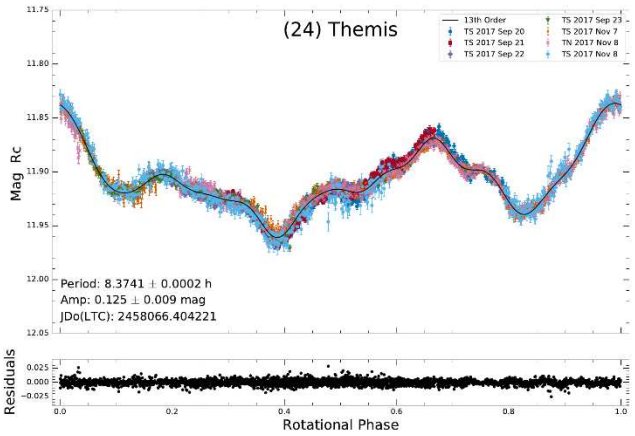

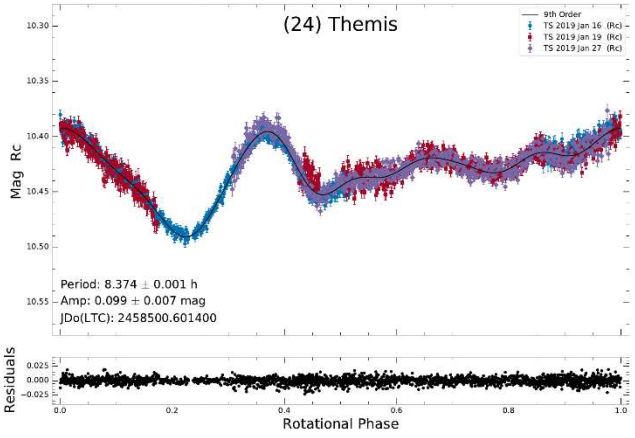

30 Urania is an S-type and with a diameter of 88 km, and it is the smallest asteroid in our sample. Its shape is irregular, and our lightcurve shows an amplitude of 0.26 mag.

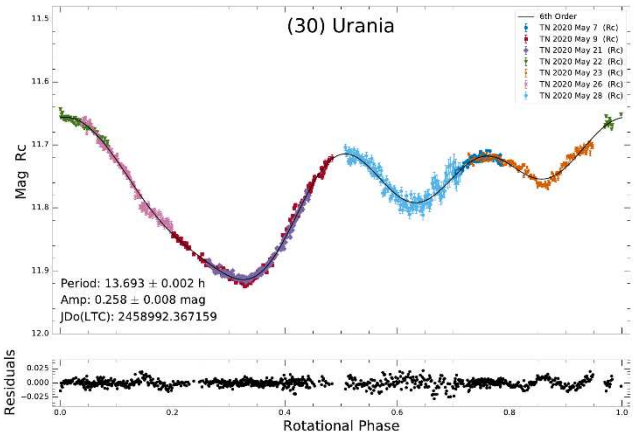

45 Eugenia is a carbonaceous asteroid with two moons. Its short rotation period of ~5.65 h was covered in one night on 2018 Mar 6.

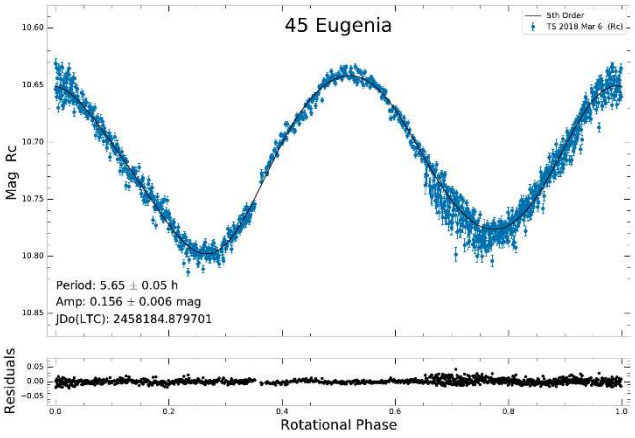

51 Nemausa is a C-type asteroid that we observed in 2019.

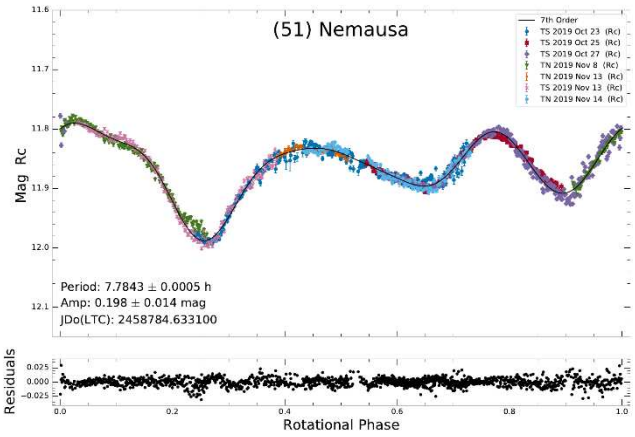

52 Europa is a C-type asteroid with a short period of ~5.58 h that was covered in one night on 2019 Aug. 26.

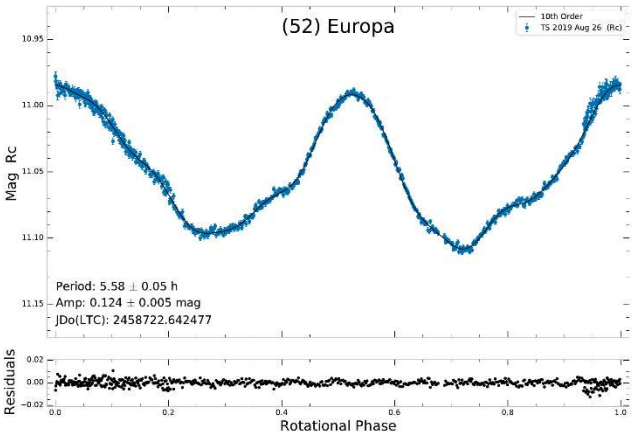

87 Sylvia is a large asteroid located in the outer region of the main belt and the first triple asteroid to be discovered (Marchis et al., 2005). Sylvia is a relatively fast rotator and has an elongated shape as shown by our lightcurve with a period of 5.1837 h and an amplitude of ~0.32 mag.

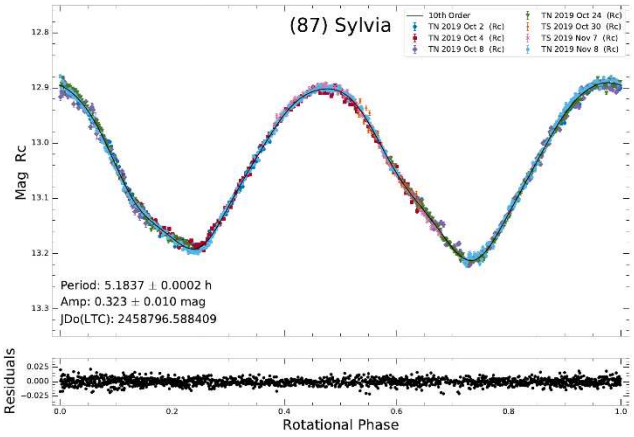

88 Thisbe is a C-type asteroid that we observed during its 2019 apparition.

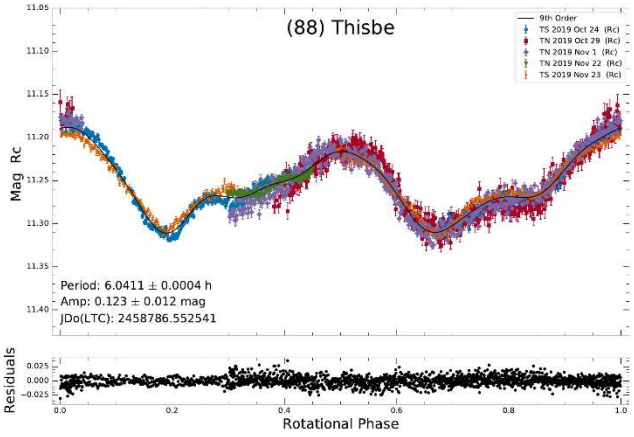

105 Artemis is a C-type asteroid with a period of ~37 h. We acquired 14 series of observations between 2020 Jan. 10 and 2020 Feb. 1 with TN and TS to fully cover its rotational lightcurve.

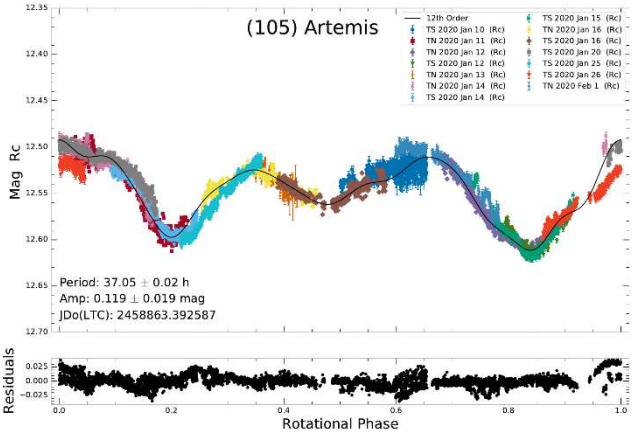

128 Nemesis is a C-type asteroid and a slow rotator. Scaltriti et al. (1979) measured a rotation period of P = 39 h and Pilcher (2015) measured a value double of that, with P = 77.81 ± 0.01 h. Recently, Colazo et al. (2022) published the period P = 38.907 ± 0.006 h. We observed Nemesis in 2021 Feb. and Mar. with TN and TS. Our analysis yields a period P = 38.904 ± 0.006 h that closely agrees with that of Colazo et al. (2022). It must be noted that our data and the shape model of Vernazza et al. (2021) favour the shorter period of ~39h but the double period still cannot be completely ruled out. Finally, we acquired BVRI sequences during five different nights to measure Nemesis' colors. The obtained color indexes are: BV = 0.406 ± 0.032, VR = 0.795 ± 0.014, VI = 0.718 ± 0.028.

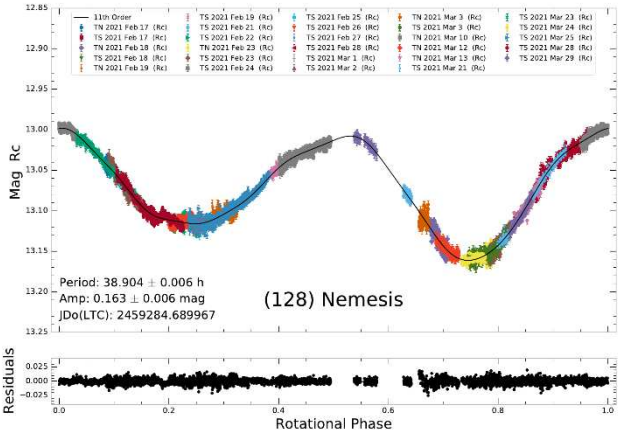

145 Adeona is a C-type asteroid that we observed in 2018. The lightcurve amplitude is small (0.064 mag) but Adeona was bright at that time with V ~11.6, resulting in good quality data.

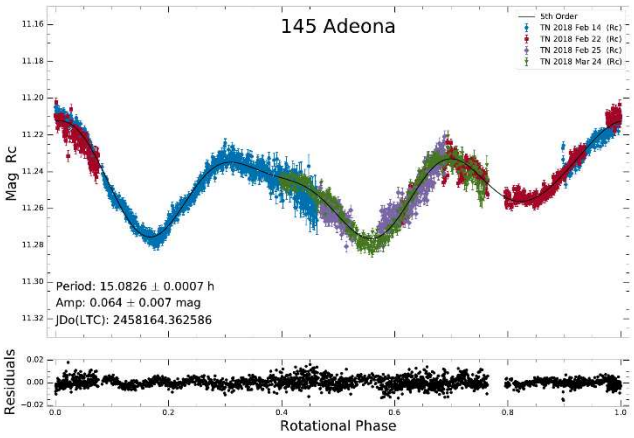

187 Lamberta. The lightcurve of this C-type asteroid was covered in two nights in May 2018 with TS.

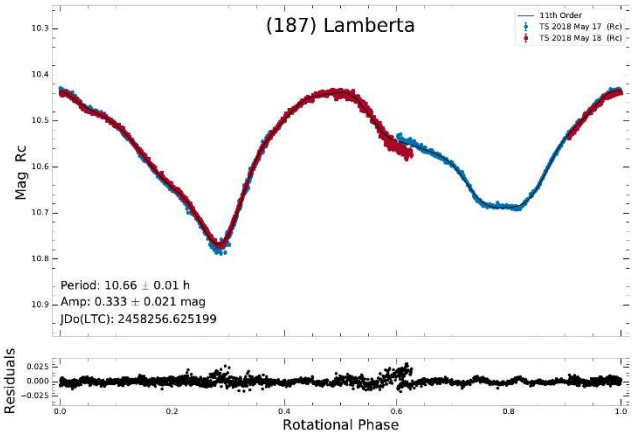

216 Kleopatra. A very smooth lightcurve was obtained from our 2021 observations of this fascinating M-type, dog-bone shaped asteroid with two moons (see e.g., Marchis et al., 2021).

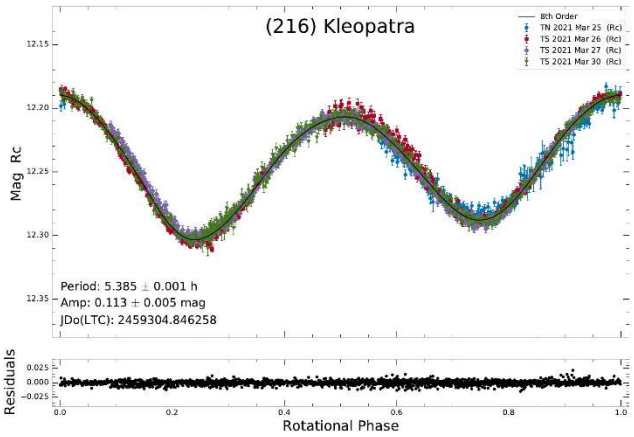

324 Bamberga is a large C-type asteroid with a regular and spherical shape. It results in small brightness changes during its rotation and makes more challenging the shape and spin axis determination. To help constrain these parameters, we regularly observed Bamberga during two months in 2019, from Feb. 19 to Apr. 18, and in Feb. 2020. In total we acquired more than 15000 data points. A spin solution was found by *SAGE* and presented in Vernazza et al. (2021).

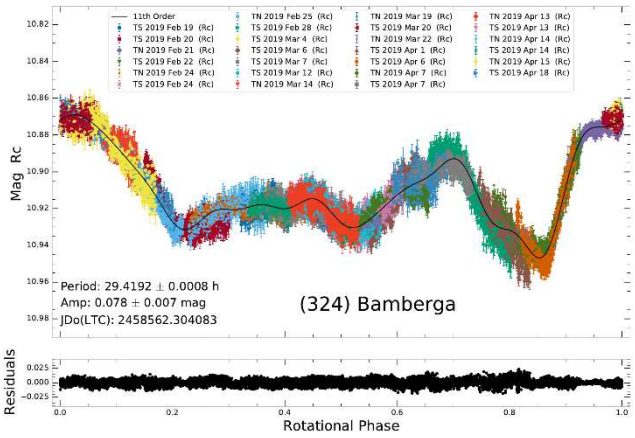

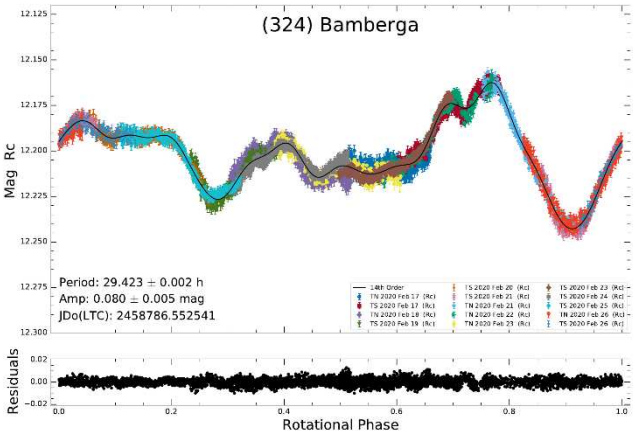

354 Eleonora is a stony asteroid that we observed in 2020 with TN. While the first four observations were taken within nine days, 19 days separate them from the last one on May 27. The solar phase angle increased from 12 to 18 degrees and the shape of the last curve has slightly changed.

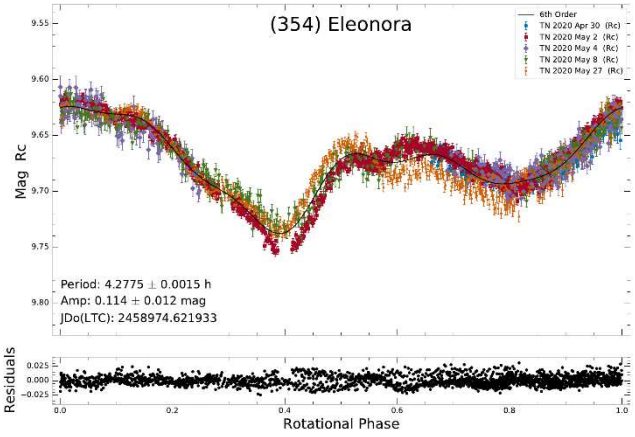

476 Hedwig. Three series of data were obtained for this long period asteroid in 2017 resulting in an incomplete lightcurve. The plot below shows the absolute magnitude H.

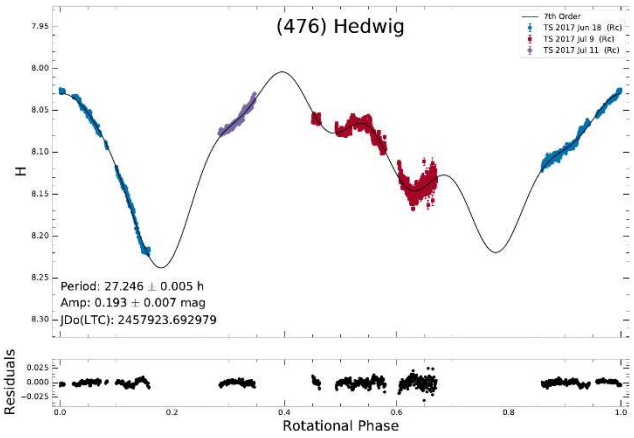

596 Scheila was observed during two nights in 2017 and more densely during its 2019 apparition. The two lightcurves show small amplitudes of 0.061 and 0.070 mag, respectively.

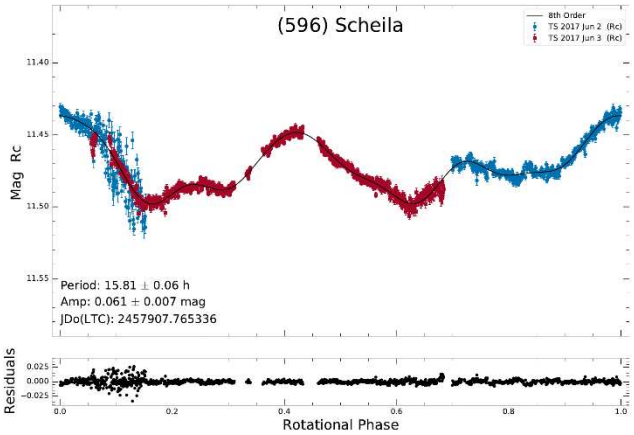

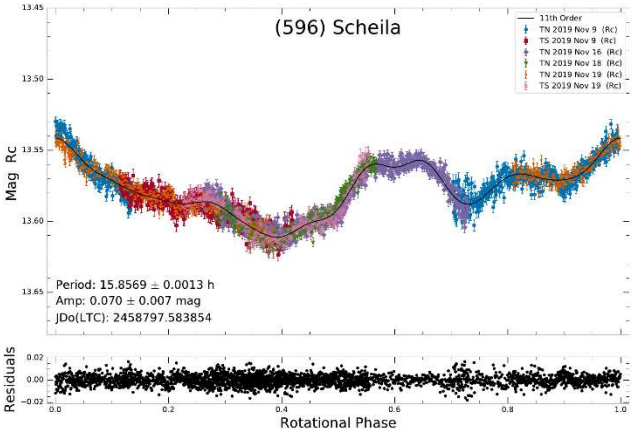

704 Interamnia is the fifth largest main-belt asteroid with a diameter of 332 km and a regular shape. We observed Interamnia in 2018 and 2019 and obtained dense lightcurves with amplitudes of 0.042 and 0.043 mag, respectively. A shape model and spin-state solution are presented in Hanuš et al. (2020).

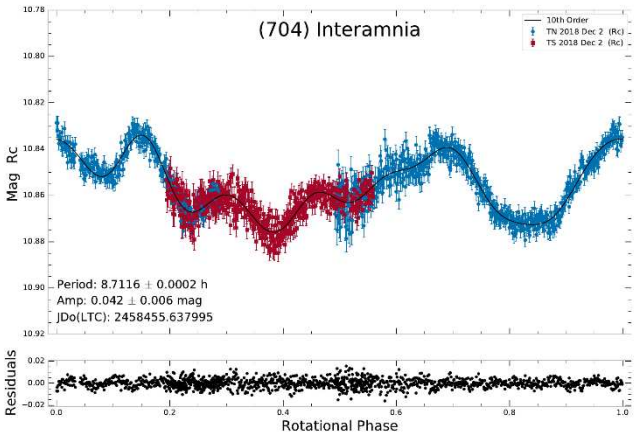

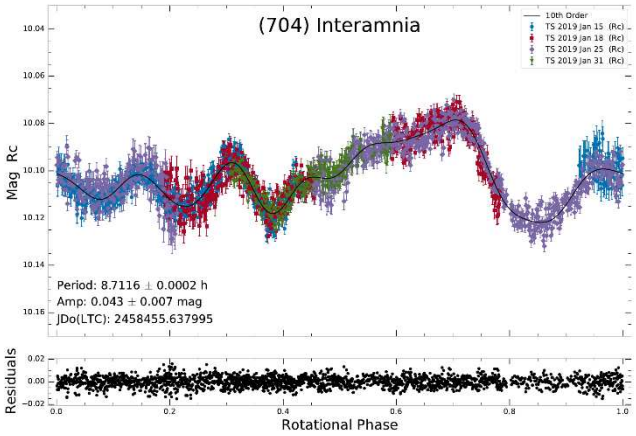

Acknowledgements

TRAPPIST is a project funded by the Belgian Fonds (National) de la Recherche Scientifique (F.R.S.-FNRS) under grant PDR T.0120.21. TRAPPIST-North is a project funded by the University of Liège, in collaboration with the Cadi Ayyad University of Marrakech (Morocco). E. Jehin is FNRS Senior Research Associate. The website of the TRAPPIST project can be visited at *https://www.trappist.uliege.be*.

References

Bartczak, P.; Dudzinski, G. (2018). "Shaping asteroid models using genetic evolution (SAGE)." *MNRAS* **473**, 5050-5065.

Colazo, M.; Morales, M.; Fornari, C.; and 21 colleagues (2022). "Photometry and Light Curve Analysis of Eight Asteroids by GORA'S Observatories." *Minor Planet Bull.* **49**, 48-51.

Elkins-Tanton, L.T.; Asphaug, E.; Bell, J.F.; and 21 colleagues (2017). "Asteroid (16) Psyche: Visiting a Metal World." *Lunar Planet. Sci. Conf.* **48**, 1718.

Ferrais, M.; Vernazza, P.; Jorda, L.; and 34 colleagues (2020). "Asteroid (16) Psyche's primordial shape: A possible Jacobi ellipsoid." *Astronomy & Astrophysics* **638**, L15.

Ferrais, M.; Jorda, L.; Vernazza, P.; and 49 colleagues (2022). "M-type (22) Kalliope: A tiny Mercury." *Astronomy & Astrophysics*, forthcoming article.

Number	Name	yyyy mm/dd	Pts	Phase	L_{PAB}	B_{PAB}	Period (h)	P.E.	Amp	A.E.
7	Iris	2020 06/26-07/10	1010	1.1, 6.1	277	2.3	7.1385	0.0015	0.21	0.01
13	Egeria	2019 08/20	1340	9.5	337	-20	7.07	0.02	0.30	0.01
15	Eunomia	2019 06/13-06/20	2681	21.0,19.8	316	3	6.083	0.001	0.46	0.04
16	Psyche	2018 08/27-09/01	1028	18.0,17.7	239	3	4.1962	0.0004	0.07	0.01
18	Melpomene	2019 08/17-08/30	1934	22.4,25.7	284	7	11.571	0.003	0.32	0.01
20	Massalia	2017 11/10-12/09	3228	15.8, 5.0	84	-1	8.0979	0.0005	0.25	0.01
20	Massalia	2019 03/14	1185	21.9	235	0	8.0979	0.0005	0.22	0.02
21	Lutetia	2019 09/11	2177	9.6	3	-4	8.16	0.05	0.16	0.01
22	Kalliope	2018 02/08-03/13	1391	10.0, 8.6	190	14	4.1485	0.0008	0.03	0.01
24	Themis	2017 09/21-11/08	3264	*9.6, 7.1	27	0	8.3741	0.0002	0.12	0.01
24	Themis	2019 01/17-01/28	2099	1.4, 6.0	113	1	8.3740	0.0010	0.10	0.01
30	Urania	2020 05/07-05/28	944	22.0,22.9	167	-2	13.693	0.002	0.26	0.01
45	Eugenia	2018 03/07	1155	5.3	177	4	5.65	0.05	0.16	0.01
51	Nemausa	2019 10/23-11/14	1478	23.4,22.7	319	5	7.7843	0.0005	0.20	0.01
52	Europa	2019 08/27	635	11.1	5	-7	5.58	0.05	0.12	0.01
87	Sylvia	2019 10/03-11/09	1557	15.1,15.2	11	26	5.1837	0.0002	0.32	0.01
88	Thisbe	2019 10/25-11/24	1966	13.5,2.4	66	4	6.0411	0.0004	0.12	0.01
105	Artemis	2020 01/11-02/01	5893	11.7,15.0	106	-27	37.05	0.02	0.12	0.02
128	Nemesis	2021 02/18-03/30	5529	18.8,17.1	235	3	38.904	0.006	0.17	0.01
145	Adeona	2019 02/14-03/24	2272	17.0,25.0	116	11	15.0826	0.0007	0.06	0.01
187	Lamberta	2018 05/17-05/18	2415	15.2,15.6	337	-9	10.66	0.01	0.33	0.01
216	Kleopatra	2021 03/26-03/31	1763	16.0,15.5	247	6	5.385	0.001	0.11	0.01
324	Bamberga	2019 02/20-03/18	10393	12.5,19.9	123	4	29.4192	0.0008	0.08	0.01
324	Bamberga	2020 02/18-02/27	5043	10.7, 8.4	185	-7	29.423	0.002	0.08	0.01
354	Eleonora	2020 05/01-05/27	2167	12.2,18.0	205	22	4.2275	0.0015	0.11	0.01
476	Hedwig	2017 06/19-07/12	1132	*6.1, 5.2	280	-2	27.246	0.005	0.19	0.01
596	Scheila	2017 06/02-06/03	1342	1.8, 2.3	249	0	15.81	0.06	0.06	0.01
596	Scheila	2019 11/09-11/20	2837	6.9, 3.5	68	-2	15.8569	0.0013	0.07	0.01
704	Interamnia	2018 12/02-12/03	1395	14.8,14.7	114	-2	8.7116	0.0002	0.04	0.01
704	Interamnia	2019 01/16-02/01	2112	2.1, 7.0	114	-6	8.7116	0.0002	0.04	0.01

Table I. Observing circumstances and results. Pts is the number of data points. The phase angles are given for the first and last date and a * indicates if it reached a minimum during the period. L_{PAB} and B_{PAB} are the approximate phase angle bisector longitude and latitude at mid-date range (see Harris et al., 1984).

Hanuš, J.; Marsset, M.; Vernazza, P.; and 35 colleagues (2019). "The shape of (7) Iris as evidence of an ancient large impact?" *Astronomy & Astrophysics* **624**, A121.

Hanuš, J.; Vernazza, P.; Viikinkoski, M.; and 56 colleagues (2020). "(704) Interamnia: a transitional object between a dwarf planet and a typical irregular-shaped minor body." *Astronomy & Astrophysics* **633**, A65.

Harris, A.W.; Young, J.W.; Scaltriti, F.; Zappala, V. (1984). "Lightcurves and phase relations of the asteroids 82 Alkmene and 444 Gyptis." *Icarus* **57**, 251-258.

Harris, A.W.; Young, J.W.; Bowell, E.; Martin, L.J.; Millis, R.L.; Poutanen, M.; Scaltriti, F.; Zappala, V.; Schober, H.J.; Debehogne, H.; Zeigler, K.W. (1989). "Photoelectric Observations of Asteroids 3, 24, 60, 261, and 863." *Icarus* **77**, 171-186.

Jehin, E.; Gillon, M.; Queloz, D.; Magain, P.; Manfroid, J.; Chantry V.; Lendl, M.; Hutsemékers, D.; Udry, S. (2011). "TRAPPIST: TRAnsiting Planets and PlanetesImals Small Telescope." *The Messenger* **145**, 2-6.

Marchis, F.; Descamps, P.; Hestroffer, D.; and Berthier, J. (2005). "Discovery of the triple asteroidal system 87 Sylvia." *Nature* **436**, 822.

Marchis, F.; Jorda, L.; Vernazza, P.; and 36 colleagues (2021). "(216) Kleopatra, a low density critically rotating M-type asteroid." *Astronomy & Astrophysics* **653**, A57.

Mommert, M. (2017). "PHOTOMETRYPIPELINE: An Automated Pipeline for Calibrated Photometry." *Astronomy and Computing* **18**, 47-53.

Pilcher, F. (2015) "New Photometric Observations of 128 Nemesis, 249 Ilse, and 279 Thule." *Minor Planet Bull.* **42**, 190-192.

Scaltriti, F.; Zappala, V.; Schober, H.J. (1979). "The Rotations of 128 Nemesis and 393 Lampetia: The Longest Known Periods to Date." *Icarus* **37**, 133-141.

Sierks, H.; Lamy, P.; Barbieri, C.; and 55 colleagues (2011). "Images of Asteroid 21 Lutetia: A Remnant Planetesimal from the Early Solar System." *Science* **334**, 487.

Tody, D. (1986). "The IRAF Data Reduction and Analysis System." *Proc. SPIE Instrumentation in Astronomy VI* **627**, 733.

Vanmunster, T. (2018). *Peranso* software. *www.cbabelgium.com/peranso/*

Vernazza, P.; Ferrais, M.; Jorda, L.; and 40 colleagues (2021). "VLT/SPHERE imaging survey of the largest main-belt asteroids: Final results and synthesis." *Astronomy & Astrophysics* **654**, A56.

Viikinkoski, M.; Kaasalainen, M.; Durech, J. (2015), "ADAM: a general method for using various data types in asteroid reconstruction." *Astronomy & Astrophysics*, **676**, A8.

Warner, B.D.; Harris, A.W.; Pravec, P. (2009). "The Asteroid Lightcurve Database." *Icarus* **202**, 134-146. Updated 2021 Dec. *http://www.MinorPlanet.info/php/lcdb.php*